J. Am. Soc. Mass Spectrom. (2017) 28:2143–2150
DOI: 10.1007/s13361-017-1742-8

RESEARCH ARTICLE

A W-Geometry Ortho-TOF MS with High Resolution and Up to 100% Duty Cycle for MS/MS

Igor V. Chernushevich,[1] Samuel I. Merenbloom,[2] Suya Liu,[1] Nic Bloomfield[1]

[1]SCIEX, Concord, ON, Canada
[2]Corning, NY, USA

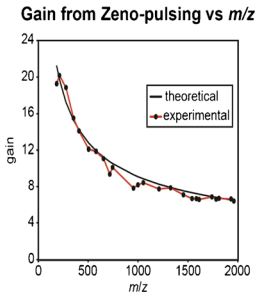

Abstract. Orthogonal injection time-of-flight (orthoTOF) mass spectrometry (MS) is the most prevalent form of TOFMS, owing to its greater control over incoming ion energy, the ability to correct for aberrations in incoming ion velocity and position, and its ability to provide an entire mass spectrum within a single scan. However, the duty cycle of orthoTOFMS is low compared with scanning analyzers, which can have 100% duty cycle when measuring a single type of ion. Typical duty cycles for orthoTOFMS range from 1% to 30%, depending on instrument geometry. Generally, as instrument resolution increases, duty cycle decreases. Additionally, the greatest duty cycle is achieved for the highest *m/z* ion recorded in the spectrum, and decreases for all other ions as a function of *m/z*. In a prior publication [Loboda, A.V.; Chernushevich, I.V. J. Am. Soc. Mass Spectrom. 20, 1342–1348 (20)], a novel trapping/release method for restoring the duty cycle of a V-geometry orthoTOFMS to near 100% (referred to as "Zeno pulsing") was presented. Here, we apply that method to a W-TOF geometry analyzer with analog detection. Across a *m/z* range of 100–2000, sensitivity gains of ~5–20 are observed, for total ion currents approaching ~10^7 ions·s^{-1}. Zeno pulsing, or similar strategies for restoring duty cycle, will continue to be important as instrument resolution in orthoTOFMS is increased through the use of ion mirrors.

Keywords: Time-of-flight mass spectrometry, Quadrupole, Collision cell, orthoTOF, Duty cycle, Mass resolution, Ion trapping, Zeno

Received: 27 March 2017/Revised: 15 June 2017/Accepted: 19 June 2017/Published Online: 17 July 2017

Introduction

Arguably the most prevalent form of time-of-flight (TOF) mass spectrometry (MS) is orthogonal injection (ortho)-TOFMS [1–4]. Orthogonal injection of ions allows greater control of both the velocity and position of incoming ions, and therefore higher resolution and mass accuracy compared with axial-injection. Furthermore, orthoTOFMS provides a spectrum of all ions within a single transient, and it is tempting to say that it is 'scanning' at a rate of >10^{11} Thomsons per s. OrthoTOFMS has been employed as a standalone analyzer [4, 5], or as part of hybrid quadrupole-TOFMS [4, 6, 7], and ion mobility spectrometry-TOFMS [8, 9] instruments. These combination instruments have found extensive use as detectors for liquid chromatography (LC) analyses [6, 8].

Despite its widespread use, orthoTOFMS suffers from a major weakness – low instrumental duty cycle that translates into low sensitivity. Duty cycle in orthoTOFMS is a function of both instrument geometry and ion *m/z*, as shown in Equation 1 [7]:

$$Duty\,Cycle\left(m/z\right) = \frac{\Delta l}{D}\sqrt{\frac{\left(m/z\right)}{\left(m/z_{max}\right)}} \quad (1)$$

where Δl is the length of the TOF accelerator window along the axis perpendicular to the TOF, D is the distance between the center of the accelerator window and the center of the detector along the same axis, m/z is the mass-to-charge of the ion of interest, and $(m/z)_{max}$ is mass-to-charge of the heaviest ion recorded in the mass spectrum. Typical values of duty cycle range from ~1 to 30%. As can be seen from Equation 1, duty cycle is greatest for ions with the largest *m/z* value in the mass spectrum, and decreases for lower *m/z*. This low duty cycle contributes to the low sensitivity of orthoTOFMS compared with scanning instruments when monitoring a single ion. Note that Equation 1 is valid only for TOF analyzers with no deflection after injection.

Correspondence to: Igor Chernushevich;
e-mail: Igor.Chernushevich@sciex.com

Additionally, there are also ion losses due to scattering on grid wires in ion mirrors that further decrease sensitivity. As long as gridded mirrors are used to increase ion flight length, and thus instrument resolution, these losses are unavoidable in TOFMS. It is worth mentioning that there are multiple approaches for high resolution (R > 100,000) TOFMS using gridless reflectors [10], sectors [11, 12], or quadrologarithmic fields [13]. However, two of these methods can only provide the highest R for a limited range of the mass spectrum [10, 11]. Although the other methods provide the highest R across the entire mass range [12, 13], both are currently theoretical, and would still be limited by low instrumental duty cycle.

Multiple attempts at increasing the duty cycle of orthoTOFMS have been presented in the literature [9, 14–20]. Perhaps the simplest method is to synchronize the pulse of the TOF accelerator to the *m/z* of interest, as demonstrated by both Whitehouse et al. [14] and by Chernushevich [15]. However, this only increases duty cycle within a limited *m/z* range. Brenton and coworkers constructed a TOF with multiple ion gates, and presented a strategy for increasing the duty cycle to 100%; again, this worked only for a limited *m/z* range [16]. Duty cycle improvement across a narrow *m/z* range has also been demonstrated for the storage and synchronized release of ions from 3D traps [17] and traveling wave ion guides [9] prior to TOFMS. A gain in signal of ~10× on average across the entire mass range has been achieved when traveling wave ion guide is synchronized with the TOF accelerator for a single peptide [18], which allowed for a 60% higher acquisition rate of tandem mass spectra compared with normal data-dependent acquisition. Hashimoto and coworkers demonstrated a duty cycle in excess of 60% across an *m/z* range of 174–1922 through a combination of two linear ion traps (LIT) and an orthoTOF [19]. However, this injection method could be operated no faster than 20 Hz, too slow to be an analyzer for LC detection.

In 2009, Loboda and Chernushevich presented a strategy for restoring the duty cycle to near 100% across the entire *m/z* range, referred to as 'Zeno pulsing' [20]. The duty cycle was restored through operating a portion of the collision cell of a QqTOF as a LIT, and trapping and releasing in a way that all ions reach the TOF accelerator at the same time. At the time of the original publication, Zeno pulsing was implemented on a QqTOF with a V-geometry (R > 20,000) and a time-to-digital converter (TDC) detector, and its control was not incorporated into data acquisition software. Here, all aspects of Zeno pulsing have been incorporated into software control, allowing us to switch between modes of operation in a rapid fashion in about 25ms, on the timescale of the LC peaks. Additionally, the TOF has been upgraded to a W-geometry (R up to 90,000) with an analog-to-digital converter (ADC) detector. In this article we present a duty cycle of nearly 100%, across an *m/z* range of 120–1961, for total ion currents approaching ~10^7 ions·s^{-1} for MS/MS. The increased duty cycle improves sensitivity for LC-MS, and Zeno pulsing (and similar techniques) will be increasingly important as we work towards higher resolution TOFMS through the use of multiple reflections, which lower the duty cycle by increasing *D* in Equation 1.

Methods

All experiments were performed on a prototype quadrupole-TOF instrument that is shown schematically in Figure 1, and that shares many similarities to the QqTOF that was described previously [20]. The most significant changes to this instrument involve the TOF analyzer. Specifically, the large ion mirror was opened to accommodate multiple passes (i.d. of

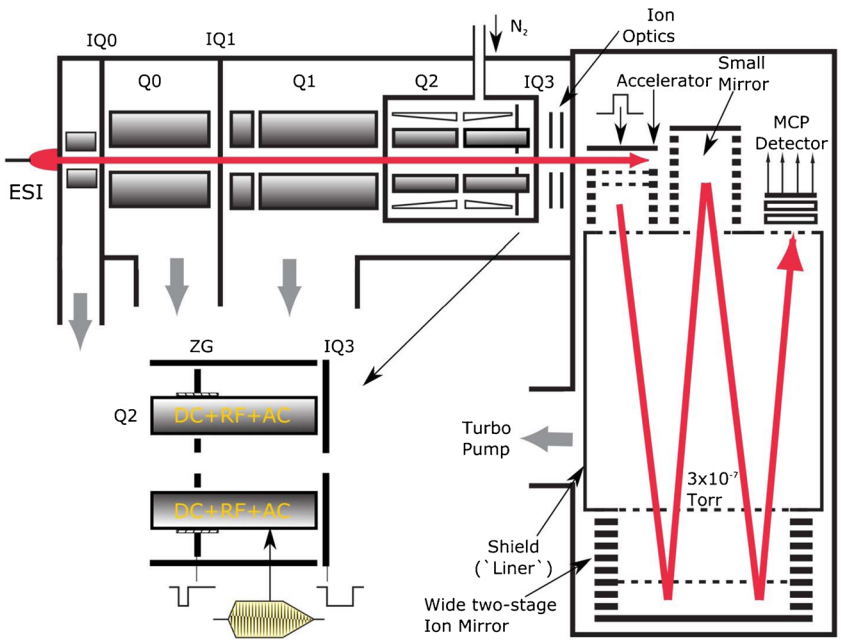

Figure 1. Scheme of the QqTOF mass spectrometer with "W-TOF" analyzer and Zeno-pulsing

grids was increased from 117 to 180 mm), and a small ion mirror (i.d. 60 mm) was inserted between the accelerator and detector, which were moved further apart from one another. The result is a W-geometry with twice the flight length, but a duty cycle 1/3 smaller than in [20], down from 24 to ~16%. The three-stage accelerator was modified to provide better field homogeneity along the ion trajectories; it accelerates ions to 15z keV.

The quadrupole ion path (with the exception of collision cell) is unchanged and is similar to that of commercially available TT6600 QqTOF instrument (Sciex, Concord, Canada). Pulsing the entrance lens IQ0 of the Q0 quadrupole ion guide introduces an artificial duty cycle (not to be mixed with TOF duty cycle!), which provides accurate control of the ion current through ion transmission coefficient (ITC) in the range from 1 to 100%. The collision cell and Zeno trap were assembled and operated as ver. 2 in [20] (same set of rods extends from collision cell into Zeno trap). Division of the Q2 rod set into two sets was dictated by required tolerances on straightness of the 4 mm diameter rods. The two rod sets are capacitively coupled, whereas DC potential on the back rods is set to be 2 to 4V more attractive. Concomitant division of the Linac rods resulted in two Linacs working in pull-push mode. Lastly, ions arriving at the four-anode detector are now recorded with a four-channel 5Gs/s 10 bit ADC (Cronologic, Germany) instead of TDC. Four channel detection provides three to four times improvement in dynamic range, higher resolution through channel 'alignment', and several other convenient options for tuning and troubleshooting.

Zeno Operation

An expanded view of the exit of the collision cell can be seen in the inset of Figure 1. In the absence of auxiliary AC (2.5 MHz), and with the appropriate DC voltages applied to the Zeno gate (ZG) and IQ3 lenses, the collision cell operates as a RF (5 MHz) ion guide in a normal, continuous introduction fashion. For duty cycle enhancement, the Zeno pulse sequence shown at the bottom of Figure 1 is applied. Briefly, ions are first trapped axially between the ZG and IQ3 lenses by switching to repulsive potentials. In the next step, the DC exit barrier is replaced by a pseudopotential well via application of auxiliary AC to the rods. The depth of the pseudopotential (U_{pseudo}) well is given by Equation 2:

$$U_{pseudo} = ze \times c \times \frac{U_{AC}^2}{\omega^2 \times \frac{m}{z}} \quad (2)$$

where z is the charge of the ion, e is the electron charge, c is a geometric constant, U_{AC} is the amplitude of the AC voltage, ω is the frequency of the AC, and m/z is the mass-to-charge of the ion. For a fixed charge state and initial AC conditions, the depth of the pseudopotential well is inversely proportional to m/z. Therefore, as the amplitude of the auxiliary AC is lowered, ions are ejected in the order from heaviest to lightest. As explained in more detail in [20], the rate at which the amplitude of the auxiliary AC is lowered can be mathematically determined so that all ions arrive at the TOF accelerator at the same time. Currently, trapping, thermalizing, and ejecting ions takes about a half of a millisecond. As a result, the TOF has to be operated at a frequency of 1.5 kHz.

As is clear from above, the auxiliary AC voltage is applied in the same phase and with nearly the same amplitude to all eight rods of collision cell, thus creating pseudopotential barrier at both ends of the collision cell. This, however, has little effect on ions entering Q2 as they approach the barrier with collision energy typically exceeding 25z eV in MS/MS mode.

Sample Preparation

Adrenocorticotropic hormone (ACTH) fragment 18–39 (*RPVKVYPNGAEDESAEAFPLEF*) and Met-enkephalin were purchased from Sigma Aldrich (Oakville, Canada) and used without any further purification. A 4 μM solution of ACTH and a 0.5 μM solution of Met-enkephalin were prepared in 49.5:49.5:1 (% v:v:v) water:methanol:formic acid, and kept refrigerated when not used for analysis. For a 'drug cocktail' of compounds with the same nominal molecular weight, separate 1 mg/mL stock solutions of bromazepam, clonazepam, oxfendazole, chlorprothixene, flusilazol, oxycodone, fendiline, and pamaquine (all from Sigma Aldrich) were prepared in water. They were then mixed and diluted to a final concentration of 100pg/μL of each compound in 49.95:49.95:0.1 (% v:v:v) water:methanol:formic acid, with the exception of bromazepam, which was diluted to 200pg/μL concentration. For electrospray ionization, solutions were infused at a flow rate of 8 $\mu L \cdot min^{-1}$.

Results and Discussion

TOF Resolution

It is widely recognized now that the way to higher resolution lies through elongating the flight path, usually by packing it into a reasonable size analyzer through multiple reflections [4]. This can be achieved either with gridded mirrors ("W-TOF" of Waters and recent "N-TOF" from Sciex), or with planar multi-reflecting TOF analyzers [10]. Increased flight path makes turn-around time – the main factor affecting resolution – smaller compared with ion flight time. Simultaneously it reduces the effect of ADC time step, which may still represent a bottleneck for mass resolution, especially at low m/z. Figure 2 demonstrates the ability to completely resolve peaks of eight compounds (drugs) having the same low nominal mass of 316 Da. Recording of such spectra of isobaric compounds is a useful test for a true resolution, and not the one achieved due to peak saturation, coalescence, or data processing. Resolution at higher masses (m/z > 800 Th) is typically around 80,000, but can be increased to 90,000 if only two middle anodes are used to record ions [21].

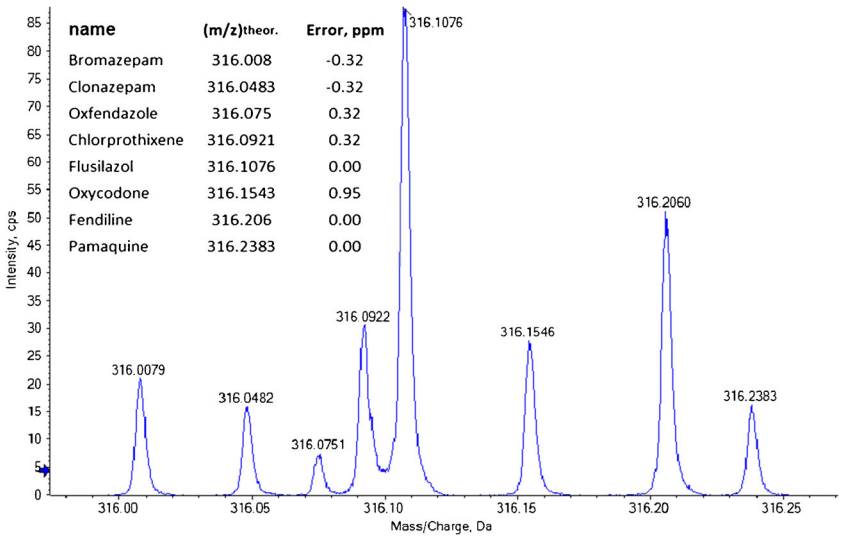

Figure 2. One-quarter Da segment of the mass spectrum of eight compounds with the same nominal *m/z* = 316 recorded with resolution (FWHM) 70,000

Resolution does come at some expense of sensitivity: geometric transmission of all the grids (92.8% transparency) passed by ions decrease from 51% (9 grids) in V-mode to 32.6% (15 grids) in W-mode – a factor of 1.57. In addition, the TOF duty cycle is reduced by 1.5 times, but this loss is almost fully recoverable through Zeno-pulsing. Finally, additional ion current reduction could happen due to imperfect focusing of low energy ion beam into the TOF extraction gap. However, 15 kV acceleration voltage in TOF and the angle required for ions to reach detector result in 'orthogonal energy' of 18.6 eV, which is relatively easy to handle.

This kind of resolution allows in some cases to resolve fine isotopic structure, in particular $XXX^{34}S^{12}C_2$ - $XXX^{32}S^{13}C_2$ combinations with Δm ~10.9 mDa. MS/MS high resolution spectrum of the third isotopic peak of Met-enkephalin (*m/z* = 576.24) is shown in Figure 3 together with its expanded views for residual precursor and several fragments. Precursor ion and all but one fragment shown in expansions clearly show partially resolved doublets, whereas the only C-terminal fragment resulted in a single peak since it does not contain any sulphur. This is an example how high resolution can help to 'read' spectra, in this case helping to distinguish between C- and N-terminal series of fragments.

Gain in MS/MS and Zeno Dynamic Range

Although Zeno pulsing can be performed theoretically all the time, it makes sense to use it during MS/MS experiments only, where ion currents are typically much lower. As well, typically ITC is used to attenuate the ion beam in TOF MS mode to prevent saturation of the detection subsystem, making it undesirable to increase signal with Zeno pulsing. Additionally, operating the TOF at a higher frequency for precursor ion surveys during LC MS experiments allows for more points to be collected along an LC peak.

It is useful to examine gain for individual ions across the entire *m/z* range. The experimentally observed gains for 24 singly charged fragment ions of the doubly charged ACTH 18–39 fragment at an ITC of 100% are compared with the theoretical gain curve in Figure 4a. For the *m/z* range across which ions are observed (120–1960), theoretical gains range from 21.2 to 6.5 (calculation of theoretical gain assumes full recovery of TOF duty cycle). All ions have experimental gains within ±16% of theory, with the b_8 ion at *m/z* 954.55 having the lowest gain compared with theory. One explanation for this observation is that this ion has sufficient internal energy to undergo further dissociation during its storage within the Zeno trap. The b_3 ion at *m/z* 353.23 has a measured gain slightly higher than theory, suggesting it is possibly a final product of the further dissociation of the excited b_8. Similarly, the y_2-H_2O (*m/z* 277.12), a_{18} (*m/z* 1932.95), and internal fragment PL (*m/z* 211.14) all have measured gains in excess of theory, suggesting they are also the products of larger fragments with excess internal energy. Although this observation could prove to be useful for probing ion energetics, it also could be a complicating factor for applications in which fragment intensity ratios are monitored. In such instances, careful control of experimental parameters, and possibly calibration of Zeno with 'thermometer ions' with well-known fragmentation thermodynamics, would be necessary.

Space Charge Effects in Zeno Trap

It is also important, however, to understand the impact of increased duty cycle and lower TOF frequency on the dynamic range of the ADC. Furthermore, it is also important to estimate the space charge capacity of the Zeno trap, and determine which would occur first, trap saturation or detector-ADC saturation.

Although a major concern with TOF duty cycle restoration is ADC saturation due to greater ion current (combined with the required operation of the TOF at lower frequency in Zeno

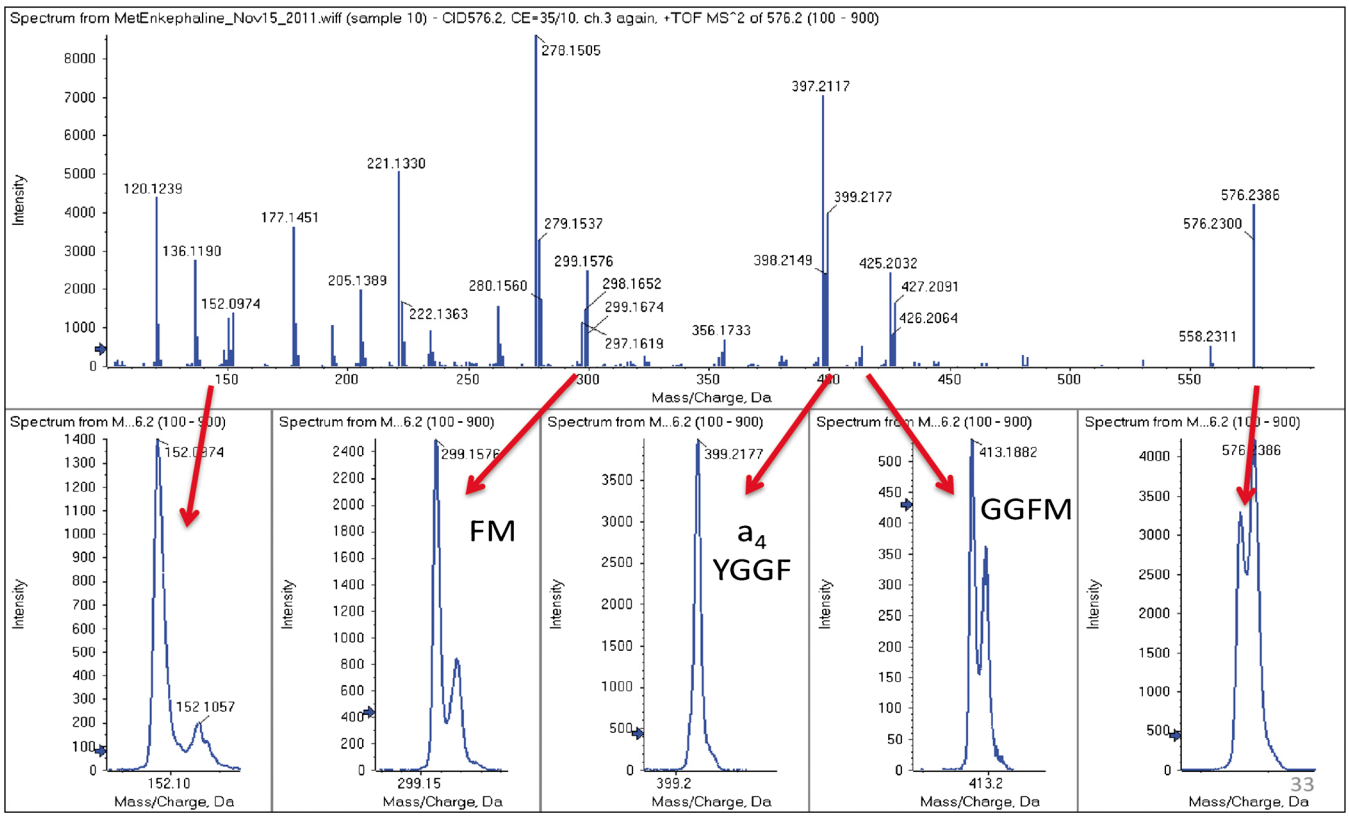

Figure 3. MS/MS spectrum of the third isotope of Met-Enkephaline (1+, *m/z* = 576.24) and segments showing fine isotopic structure of the remaining precursor and several fragments; recorded with two middle anodes, resolution ~90,000 (FWHM)

pulsing mode), another concern is whether or not the Zeno trap can store and transfer enough charges. For this experiment, we electrosprayed adrenocorticotropic hormone (ACTH) fragment 18–39 from a 4 μM solution, and performed MS/MS of the doubly charged ion at *m/z* = 1233, generating fragments from *m/z* 120 to1960. To increase ion current, we changed the ITC from 2% to 100%. The ITC controls the introduction of ions from the source into the resolving quadrupole and ultimately the collision cell; the duty cycle of the TOF analyzer is not at all affected. In the normal mode of operation, the total ion current (TIC) increased linearly with increasing ITC, all the way to 100%, or just over half a million ions·s^{-1} (Figure 4b). Additionally, ion signal is distributed rather evenly (+/−10%) across the four anodes of our detector, with slightly more on the middle two anodes, regardless of ITC (not shown).

In Zeno pulsing mode, a small portion of the collision cell, specifically the volume between the "Zeno Gate" and IQ3 lenses is used for ion storage. The same number of ions has to be stored for almost a millisecond in a much smaller 10 mm long trapping region. Initially, in Zeno mode, TIC increased linearly until ~2 million ions·s^{-1}. Upon further inspection, it was observed that although lower *m/z* ions maintained gains close to theoretical values with increasing ITC, higher *m/z* ions had decreasing gains with increasing ion current. Therefore, we suspected that this was due to space charge effects, and not ADC saturation. Because the height of the pseudopotential well is inversely proportional to ion *m/z* (Equation 2), ions with the highest *m/z* values are affected most by a decrease in the pseudopotential well depth and/or an increase in internal energy. Therefore, ions with the highest *m/z* values are the first ions ejected as space charge increases within the trap. This theory was tested with the four anode 'display meter'.

The detector of the TOF analyzer is divided into four sections that are arranged parallel to the direction of ion acceleration into the TOF. Anodes are numbered such that successive anodes are further away from the TOF accelerator along this axis. After traveling through the analyzer, the ion packet is approximately 40 mm long in the direction in which ions enter the TOF accelerator. The total length of the four anodes combined is 40 mm, with anodes one and four being slightly larger than anodes two and three (12 mm versus 8 mm). The distribution of ions across the four anodes provides information regarding both the position and the energy of ions in the ion packet. Originally, collision cell potentials were tuned so that ion signal at low ITC was centered on anodes 2 and 3 in Zeno mode (Figure 5a). As ITC was increased, the ion signal (mostly for those over *m/z* 1800) migrated to higher anodes (Figure 5b), confirming that higher *m/z* ions were being prematurely ejected due to space charge effects. At a high enough number of charges, high *m/z* ions were ejected too early to be pulsed into the analyzer and observed on the detector, resulting in the decreasing gain at higher *m/z* with increasing ITC.

DC potentials at the exit of the collision cell and the amplitude of the Zeno AC were retuned so that ions were observed

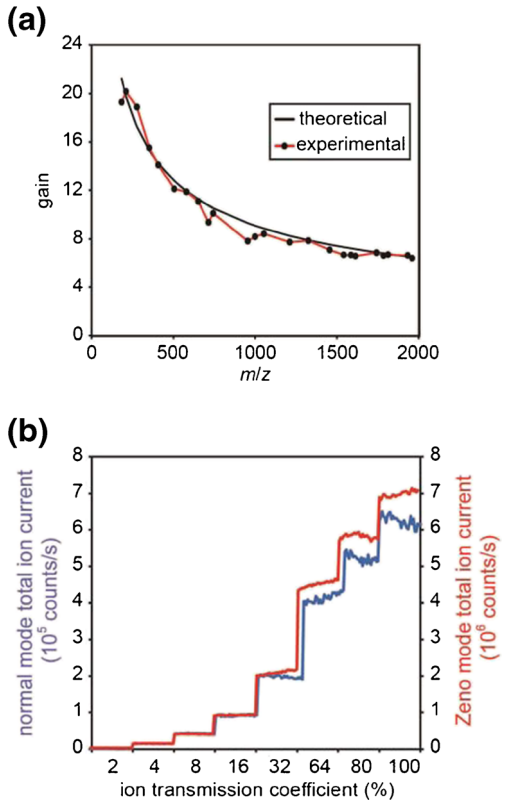

Figure 4. (**a**) Theoretically predicted and experimental gain from Zeno-pulsing as a function of *m/z* of the fragments. Data extracted from MS/MS spectra of ACTH fragment 18–39 recorded with and without Zeno-pulsing. (**b**) Linearity test: total ion current (TIC) measured as a function of ion transmission coefficient (ITC) in normal (blue) and in Zeno-pulsing mode (red)

predominantly on anodes 1, 2, and 3 (Figure 5c). As observed previously, signal for higher *m/z* ions migrated to higher anodes with increasing ITC (Figure 5d). However, signal migrated across an observable region of the detector, as opposed to away from the detector surface. The net result is gain within several percent of theory across the entire mass range, and a linear increase in signal up to just over 7 million ions·s^{-1}. Taking into account the frequency of TOF operation, and estimating losses to slits (×3) and grids (×3.1), the Zeno trap can reliably store and deliver around 4 × 10^4 ions per experiment. Retaining signal linearity well beyond this point would likely require redesign of the collision cell.

A simple test of Zeno pulsing operation is to compare the total ion current (TIC) in Zeno pulsing mode to the TIC in normal operation. Observing this ratio combined with increasing the ion current through the ITC examines the dynamic range of both the Zeno trap and the ADC. Plots of the TIC as a function of ITC for the MS/MS of ACTH fragment 18–39 with either normal continuous transmission or Zeno pulsing are shown in Figure 4b. For the *m/z* range across which ions are observed (120–1960), theoretical weighted average gain is about ~10.5×. Observed average gains are within ±15% of theory, with a low of 8.9× at an ITC of 8% and a high of 11.3× at an ITC of 2%. Average gains greater than theory can be due to low signal-to-noise in normal operation (particularly at lower ITC values), enhanced fragmentation in Zeno pulsing due to the combined ion heating from the Zeno AC and greater ion storage time, and/or differences in the 'price' assigned to an individual ion by the ADC varying slightly with ion flux. Although a few items can be improved upon, Figure 4b shows that the current combination of Zeno pulsing and ADC detection is capable of operating within ±15% of theory up to ~7·10^6 ions·s^{-1}, or approximately 4 × 10^4 ions per single trapping/extraction cycle (assuming losses to slits ×3 and grids ×3.1, and extraction frequency of 1.5 kHz).

For applications in which greater duty cycle and signal-to-noise alone are beneficial, particularly at low *m/z*, Figure 4 demonstrates that Zeno pulsing combined with analog detection can provide dynamic range of nearly seven orders of magnitude.

Applications

To test the benefits of Zeno pulsing and high resolution on real world applications, *E. coli* cell lysate tryptic digests were purchased from Waters (Milford, MA, USA, 01757, product

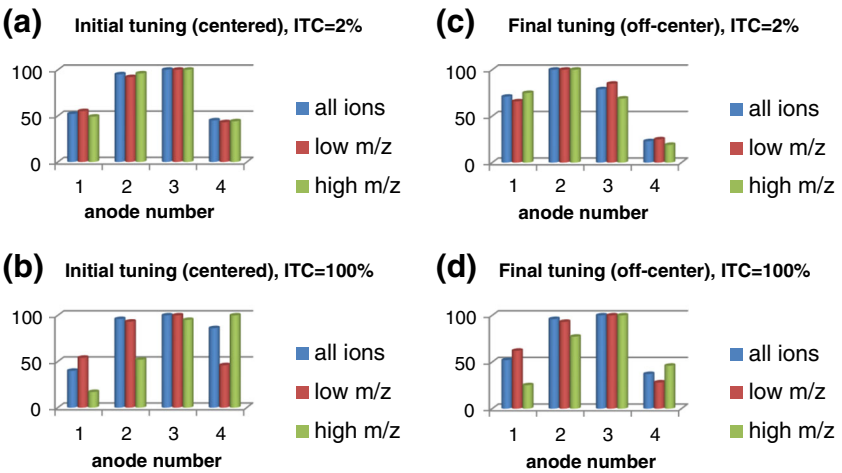

Figure 5. Ion distribution between anodes. Fragment ions of 2+ ion of ACTH, *m/z* = 1233.1. "All ions" – *m/z* from 120 to 2000; "low *m/z*" – *m/z* from 120 to 500; "high *m/z*" – *m/z* from 1800 to 2000

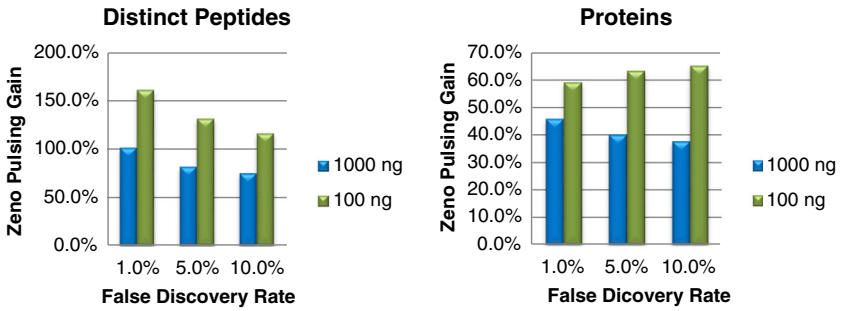

Figure 6. Relative gains from Zeno pulsing at different sample loads

no: 186003196). Lyophilized *E. coli* sample was dissolved in 2% acetonitrile in water containing 0.1% formic acid at concentration of 333 ng/µL or 33.3 ng/µL.

E. coli cell lysate samples were analyzed using the Eksigent nanoLC-Ultra 2D system combined with the cHiPLC nanoflex system (both from Sciex, Concord, Canada) in a Trap-Elute mode. The samples (3 µL) were first loaded on the cHiPLC trap column (200 µm × 500 µm, ChromXP C18-CL, 3 µm, 300 Å) and desalted at a flow rate of 2 µL/min. Then, the sample was eluted to and separated on a nano cHiPLC column (75 µm × 15 cm, ChromXP C18-CL, 3 µm, 300 Å) with a gradient of 12%–35% acetonitrile (0.1% formic acid) in 57 min. The total nanoLC time was 100 min including sample loading, desalting, and elution.

The effluent from nano LC was analyzed on a QqTOF instrument with a Zeno enhanced collision cell and W TOF geometry as described above via the NanoSpray III source. The analysis was done with an information-dependent acquisition method. The method consists of a TOF MS survey scan of 250 ms covering *m/z* 400–1800 recorded in normal mode with dynamic ITC, followed by up to 20 MS/MS per cycle with a 50 ms accumulation time covering *m/z* 100–1800. All runs were done in high resolution mode. Switching time between the two modes was less than 25 ms. Q1 resolution was set to unit. Rolling collision energy spread of 15 V was used. All data were processed using ProteinPilot Software 4.5 beta with integrated false discovery rate analysis. The same parameter settings were used for all data acquired.

Samples corresponding to 1000 ng and 100 ng injections were analyzed in triplicate with Zeno pulsing on and Zeno pulsing off. The number of peptides and proteins identified are compared in Tables 1 and 2, and Figure 6. Clearly, higher intensity of MS/MS spectra in Zeno pulsing mode yields in identification at both the peptide level and the protein level. The absolute numbers of proteins identified are not the highest we have ever observed on comercial QqTOF instruments when injecting the Waters *E. coli* standard but this can be explained by the fact that high resolution mode rather than high sensitivity MS/MS mode was used, as well as extra grid losses related

Table 1. Protein/Peptide LC-MS/MS Identification (ProteinPilot) for 1000 ng Injection with and without Zeno Pulsing

Data level	FDR	Zeno 3	Zeno 2	Zeno 1	Zeno off 3	Zeno off 2	Zeno off 1	Average gain
Protein	1.00%	894	898	884	563	624	648	45.80%
Protein	5.00%	917	918	890	625	670	651	40.00%
Protein	10.00%	926	927	894	655	690	651	37.60%
Distinct peptides	1.00%	7456	7838	8139	3836	4117	3698	101.10%
Distinct peptides	5.00%	8921	9093	9364	5010	5151	4901	81.80%
Distinct peptides	10.00%	9506	9663	9869	5515	5603	5471	75.00%
Spectra acquired	N/A	38367	34430	37445	35504	34932	34420	5.14%

FDR = false discovery rate.

Table 2. Protein/Peptide LC-MS/MS Identification (ProteinPilot) for 100 ng Injection with and without Zeno Pulsing

Data level	FDR	Zeno 3	Zeno 2	Zeno 1	Zeno off 3	Zeno off 2	Zeno off 1	Average gain
Protein	1.00%	487	540	517	325	307	338	59.20%
Protein	5.00%	523	565	542	326	334	338	63.30%
Protein	10.00%	540	576	554	326	347	338	65.20%
Distinct peptides	1.00%	2693	2786	2762	1031	1025	1099	161.20%
Distinct peptides	5.00%	3414	3537	3482	1469	1493	1545	131.50%
Distinct peptides	10.00%	3782	3894	3795	1750	1773	1784	116.10%
Spectra acquired	N/A	22839	22732	22741	21489	21384	21326	6.40%

FDR = false discovery rate.

to W-geometry, together costing about a factor of four in sensitivty. Given these considerations, Zeno pulsing may be used in combination with W-geometry to gain high resolution without losing sensitivity, or Zeno pulsing could be used in V- or N-geometry to yield ultra high sensitivity. For precious samples lower loads could be used while still maintining depth of coverage. Our data clearly show higher percentage gains at lower sample loads. Future experiments will target testing Zeno pulsing in V- and N-geometry to lower the absolute level of protein identification.

Conclusion

The current trend of gaining higher resolution of orthoTOF analyzers through increased number of reflections results inevitably in drastic reduction of the duty cycle and, hence, sensitivity. "Zeno-pulsing" offers a reliable way for almost complete (within 15%) restoration of duty cycle with no 'side effects' on resolution and no mass discrimination. Owing to increased signal and reduced dynamic range in this mode, Zeno-pulsing is applied in MS/MS mode only, when ion current is lower. The 10 mm long Zeno trap can operate quantitatively even under high space charge conditions – at and above 40,000 charges per transient corresponding to TIC of >5,000,000 counts/s. ADC is a requirement under these conditions. Software switches automatically between single MS in normal continuous introduction mode and MS/MS in Zeno-trapping mode.

Acknowledgements

The authors are indebted to Alexander (Sasha) Loboda for valuable discussions and advice at the early stages of this project. They are grateful to Slobodan Marinkovic for mechanical design of W-TOF analyzer, John Vandermey, Tom Binko, and Matt Romaschin for electronics for Zeno-pulsing, Mircea Toca for help in mechanical emergencies, and Xiang Gao and George Davydenko for help with software.

References

1. Dodonov, A.F., Chernushevich, I.V., Laiko, V.V.: Electrospray ionization on a reflecting time-of-flight mass spectrometer. In: Cotter, R.J. (ed.) Time-of-flight mass spectrometry, pp. 108–123. Am. Chem. Soc. Symposium Series 549, Washington, DC (1994)
2. Verentchikov, A.N., Ens, W., Standing, K.G.: Reflecting time-of-flight mass spectrometer with an electrospray ion source and orthogonal extraction. Anal. Chem. **66**, 126–133 (1994)
3. Guilhaus, M., Selby, D., Mlynski, V.: Orthogonal acceleration time-of-flight mass spectrometry. Mass Spectrom. Rev. **19**, 65–107 (2000)
4. Radionova, A., Filippov, I., Derrick, P.J.: In pursuit of resolution in time-of-flight mass spectrometry: a historical perspective. Mass Spectrom. (2015). doi:10.1002/mas.21470
5. Chernushevich, I.V., Ens, W., Standing, K.G.: Orthogonal injection TOF MS for analyzing biomolecules. Anal. Chem. **71**, 452A–461A (1999)
6. Morris, H.R., Paxton, T., Dell, A., Langhorne, J., Berg, M., Bordoli, R.S., Hoyes, J., Bateman, R.H.: High sensitivity collisionally-activated decomposition tandem mass spectrometry on a novel quadrupole/orthogonal-acceleration time-of-flight mass spectrometer. Rapid Commun. Mass Spectrom. **10**, 889–896 (1996)
7. Chernushevich, I.V., Loboda, A.V., Thomson, B.A.: An introduction to quadrupole-time-of-flight mass spectrometry. J. Mass Spectrom. **36**, 849–865 (2001)
8. Bohrer, B.C., Merenbloom, S.I., Koeniger, S.L., Hilderbrand, A.E., Clemmer, D.E.: Biomolecule analysis by ion mobility spectrometry. Annu. Rev. Anal. Chem. **1**, 293–327 (2008)
9. Pringle, S.D., Giles, K., Wildgoose, J.L., Williams, J.P., Slade, S.E., Thalassinos, K., Bateman, R.H., Bowers, M.T., Scrivens, J.H.: An investigation of the mobility separation of some peptide and protein ions using a new hybrid quadrupole/traveling wave IMS/oa-ToF instrument. Int. J. Mass Spectrom. **261**, 1–12 (2007)
10. Yavor, M., Verentchikov, A., Hasin, J., Kozlov, B., Gavrik, M., Trufanov, A.: Planar multi-reflecting time-of-flight mass analyzer with a jig-saw ion path. Phys. Procedia **1**, 391–400 (2008)
11. Toyoda, M., Okumura, D., Ishihara, M., Katakuse, I.: Multi-turn time-of-flight mass spectrometers with electrostatic sectors. J. Mass Spectrom. **38**, 1125–1142 (2003)
12. Shchepunov, V., Rignall, M., Giles, R., Nakanishi, H.: "A High Resolution Multi-turn TOF Mass Analyzer" poster presentation at the 63rd annual ASMS Conference, May 31–June 4, St. Louis, MO (2015)
13. Richardson, K., Hoyes, J.: A novel multipass oa-TOF mass spectrometer. Int. J. Mass Spectrom. **377**, 309–315 (2015)
14. Whitehouse, C.M., Guilcicek, E., Andrien, B., Banks, F., Mancini, R.: A two-dimensional ion trap API TOF mass spectrometer. Proceedings of the 46th ASMS Conference on Mass Spectrometry and Allied Topics, p. 39. Orlando, FL (1998)
15. Chernushevich, I.V.: Duty cycle improvement for a QqTOF mass spectrometer and its use for precursor ion scanning. Eur. Mass Spectrom. **6**, 471–479 (2000)
16. Brenton, A.G., Krastev, T., Rousell, D.J., Kennedy, M.A., Craze, A.S., Williams, C.M.: Improvement of the duty cycle of an orthogonal acceleration time-of-flight mass spectrometer using ion gates. Rapid Commun. Mass Spectrom. **21**, 3093–3102 (2007)
17. . Okumura, A., Hirabayashi, A., Baba, T., Hashimoto, Y., Waki, I., Yoshinari, K.: Orthogonal trap-TOF mass spectrometer (1) – Synchronous coupling of trap and TOF. Proceedings of the 51st ASMS Conference on Mass Spectrometry and Allied Topics. Montreal, Quebec, Canada (2003)
18. Helm, D., Vissers, J.P.C., Hughes, C.J., Hahne, H., Ruprecht, B., Pachl, F., Grzyb, A., Richardson, K., Wildgoose, J., Maier, S.K., Marx, H., Wilhelm, M., Becher, I., Lemeer, S., Bantscheff, M., Langridge, J.I., Kuster, B.: Ion mobility tandem mass spectrometry enhances performance of bottom-up proteomics. Mol. Cell Proteom. **12**, 3709–3715 (2014)
19. Hashimoto, Y., Hasegawa, H., Satake, H., Baba, T., Waki, I.: Duty cycle enhancement of an orthogonal acceleration mass spectrometer using an axially-resonant excitation linear ion trap. J. Am. Soc. Mass Spectrom. **17**, 1669–1674 (2006)
20. Loboda, A.V., Chernushevich, I.V.: A novel ion trap that enables high duty cycle and wide *m/z* range on an orthogonal injection TOF mass spectrometer. J. Am. Soc. Mass Spectrom. **20**, 1342–1348 (2009)
21. Merenbloom, S.I., Bloomfield, N., LeBlanc, Y., Loboda, A.V., Chernushevich, I.V.: A W-geometry ortho-TOF MS with high resolution and up to 100% duty cycle for MS/MS. Proceedings of the 63rd ASMS Conference on Mass Spectrometry and Allied Topics, St. Louis, MO (2015)